

# MALAYSIAN JOURNAL OF ANALYTICAL SCIENCES

Published by The Malaysian Analytical Sciences Society

ISSN 1394 - 2506

# $TiO_2$ DOPED WITH $Fe_2O_3$ FOR PHOTOELECTROCHEMICAL WATER SPLITTING ELECTRODE: EXPERIMENTAL AND DENSITY FUNCTIONAL THEORY STUDY

(TiO<sub>2</sub> Di Dop Bersama Fe<sub>2</sub>O<sub>3</sub> untuk Elektrod Pembelahan Molekul Air Secara Fotoelektrokimia: Eksperimen dan Kajian Teori Fungsi Ketumpatan)

Khuzaimah Arifin<sup>1\*</sup>, Hasmida Abdul Kadir<sup>1,3</sup>, Lorna Jeffery Minggu<sup>1</sup>, Wan Ramli Wan Daud<sup>1,2</sup>, Mohammad B. Kassim<sup>1,3</sup>

<sup>1</sup>Fuel Cell Institute

<sup>2</sup>Department of Chemical and Process Engineering

<sup>3</sup>School of Chemical Sciences and Food Technology, Faculty of Science and Technology

Universiti Kebangsaan Malaysia, 43600 UKM Bangi, Selangor, Malaysia

\*Corresponding author: khuzaim@ukm.edu.my

Received: 5 February 2016; Accepted: 22 April 2016

# Abstract

Various modifications of the titanium dioxide thin films have been done in fulfilling the photoelectrode requirements for photoelectrochemical water splitting reaction. In this study, surface passivation of  $TiO_2$  by hematite- $Fe_2O_3$  was reported. Electrodeposition technique was used to deposit the  $Fe_2O_3$  onto the  $TiO_2/FTO$  film with variation of time. X-ray diffraction (XRD), Scanning Electron Microscope (SEM) and UV-Vis spectroscopic analyses were used to characterize the electrode. Plane-wave-based pseudopotential density functional theory (DFT) calculations were used to analyze the electronic structure and charge potential at the surface of the electrode. The photocurrent measurement showed that current density of  $TiO_2/Fe_2O_3$  electrode was higher than the  $TiO_2/FTO$  under the same illumination intensity of  $100 \text{ mWcm}^{-2}$ . The highest current density was produced by 5 minutes electrodeposition of  $Fe_2O_3$ , which also shifted the absorption to visible region at the threshold wavelength of 518 nm.

Keywords: titanium dioxide, iron(III) oxide, passivation layer, band gap

#### Abstrak

Pelbagai pengubahsuaian titanium dioksida filem nipis telah dilakukan untuk memenuhi keperluan fotoelektrod bagi tindak balas fotoelektrokimia pembelahan molekul air. Dalam kajian ini, dilaporkan pempasifan permukaan TiO<sub>2</sub> dengan bijih besi-Fe<sub>2</sub>O<sub>3</sub>. Teknik pengelektroenapan digunakan untuk mendepositkan Fe<sub>2</sub>O<sub>3</sub> ke TiO<sub>2</sub>/FTO filem dengan pelbagai masa pengelektroenapan. Analisis XRD, SEM dan UV-Vis spektroskopi telah digunakan untuk mencirikan elektrod. pengiraan teori fungsi ketumpatan (DFT) berasaskan planar gelombang pseudopotential telah digunakan untuk menganalisis struktur elektronik dan potensi caj di permukaan elektrod. Pengukuran arusfoto menunjukkan bahawa ketumpatan arus TiO<sub>2</sub>/Fe<sub>2</sub>O<sub>3</sub> elektrod adalah lebih tinggi daripada TiO<sub>2</sub>/FTO bawah keamatan pencahayaan yang sama, 100 mWcm<sup>-2</sup>. Ketumpatan semasa tertinggi dihasilkan oleh 5 minit pengelektroenapan Fe<sub>2</sub>O<sub>3</sub>, yang mana penyerapan beralih ke kawasan yang boleh dilihat pada panjang gelombang ambang 518 nm.

Kata kunci: titanium dioksida, ferum (III) oksida, lapisan pasif, sela jalur

#### Introduction

Hydrogen has been considered as an alternative fuel to replace fossil fuels for many years. It is used in fuel cell technology to generate electricity where water molecule is the only byproduct [1]. Hydrogen is plentiful in the universe, obtained via extraction off water molecule, an element, which is abundant and cheap; however requires a lot of energy to extract it. One of the promising method to produce hydrogen from water molecule is through photoelectrochemical (PEC) reaction that utilizes sunlight energy [2]. The system uses inexpensive metal oxide photoelectrode without the expense of electrolyzer, which leads to a further reduction in the cost of hydrogen delivery. The concept was first demonstrated by Honda and Fujishima in 1972 and since then, its science has influenced many followers [3].

PEC cell is a type of an electrolytic cell, where the sunlight is absorbed by the photoelectrode to generate current that is used to drive an electrochemical reaction. Generally, photoelectrode is an n or a p-type semiconductor electrode, which flows the electrons generated by the light induced chemical reactions initiated at its surface. Several photoelectrode requirements that must be fulfilled for direct PEC water splitting to occur are listed in Table 1. The band gap of photoelectrode semiconductor must be at least 1.5 eV, higher than the effective redox potential of water, which is about 1.23 - 1.4 eV [4.5].

Condition	Requirement
PEC water-splitting	$H_2O_{(liquid)} + 2h\upsilon \rightarrow \frac{1}{2}O_{2(gas)} + H_{2(gas)}$
Minimum potential	$E^{\circ}_{H_2O}(25 \ ^{\circ}C)_{min} = 1.229 \ eV$
Practical potential	$E^{\circ}_{H_2O}(25  {}^{\circ}C)_{prac} = 1.6 - 2.0  eV$
(+overpotential & losses)	$E_{bandgap} > E^{\circ}_{H_2O}$
Utilization of sunlight	UV > hv (Vis) > IR
	$h\nu \ge E_{bandgap}$
Bandedges	$C_{band\ edge} < E^{\circ}_{H2/H^{+}}$
	$V_{band\ edge} > E^{\circ}_{O2/H2O}$

Table 1. Main PEC water-splitting requirements [4]

Concurrently, the semiconductor's conduction band (CB) must be higher than the reduction potential of water, whle its valence level (VB) must be lower than the oxidation potential of water. The focus of recent PEC research are mostly on developing photoelectrode materials that meet with the criteria besides high efficiencies, low-cost, long-term usages and non-photocorrosion of materials [3].

Titanium dioxide (TiO<sub>2</sub>) is reported as the most promising photoelectrode [6]. This material has several advantages for photochemistry and photo-electrochemistry including low cost, widely available, non-photocorrosion and nontoxic. However, TiO<sub>2</sub> photocatalytic has large band gaps that limit its absorption of solar radiation to just 4 %, which is of UV spectrum. Numerous attempts have been made to expand the TiO<sub>2</sub> photoanode absorption spectrum to longer wavelengths: through doping TiO<sub>2</sub> with various metals and anions, use a dye-sensitizer molecule [7] and also morphology modifications of nano-scaled TiO<sub>2</sub>, namely spheres, wires, rods and tubes [8, 9]. Significant experimental results are also observed by a surface passivation layer of TiO<sub>2</sub> with various metal oxide [10, 11]. Surface passivation layers electrode is a type of junction electrode, which comprises two or more layers of semiconductors. The surface passivation layers provide an alternative low energy route for charge transfer through catalytically active sites. In addition, surface passivation layers can reduce corrosion and improve chemical or photochemical stability of photoelectrode when immersed in an electrolyte [3,12].

In designing the passivation layer, it is important to consider the band positions of the metal oxides (Figure 1). For wide band gap semiconductor,  $TiO_2$  should be combined with a narrow band gap metal oxide:  $WO_3$  [13],  $Cu_2O$ 

[14], CdTe [15] and CdS [16], that can absorb visible light. Here, investigation TiO<sub>2</sub> passivated by hematite-Fe<sub>2</sub>O<sub>3</sub> is reported. Fe<sub>2</sub>O<sub>3</sub> is one of prospective material for PEC. It is a photoactive material and absorbs visible light, however is poor in conductivity and has a CB energy below the reduction potential of hydrogen ion [11].

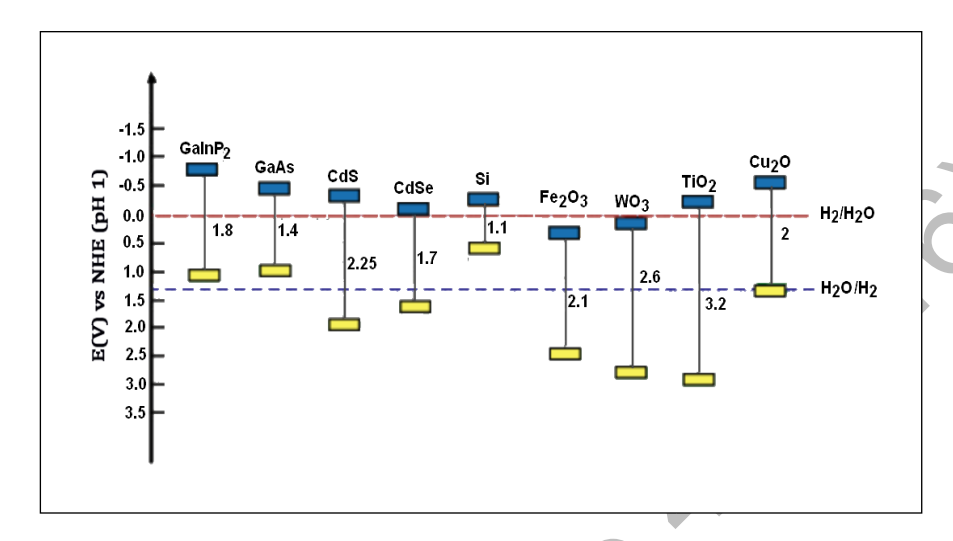


Figure 1. Bandgap and band edges of some semiconductor materials compared with a redox potential of water molecules

In this study, the  $Fe_2O_3$  was electrodeposited on the  $TiO_2$ /FTO thin film by variation of time. The  $Fe_2O_3$ /TiO<sub>2</sub>/FTO multilayer film system was characterized by X-ray diffraction (XRD), Scanning Electron Microscope (SEM) and Uv-vis spectroscopy. PEC performance was measured by calculating its I-V under UV-vis light illumination.

# **Materials and Methods**

#### Photoelectrode preparation

The TiO<sub>2</sub> electrodes were prepared using commercial colloidal TiO<sub>2</sub> powder (Degussa P25) by doctor-blading onto fluorine-doped tin oxide (FTO) glass plates. The 1 g TiO<sub>2</sub> powder was ground with 1 ml dipolyethylene glycol 300 (Merck), Triton-X and double-distilled water to form homogenous paste. The paste was smeared onto a clean FTO glass. Then, the TiO<sub>2</sub>/FTO was dried at room temperature for a few minutes and was heated in a furnace at 450 °C for 2 hours with ramping rate of 5 °C s<sup>-1</sup>. Afterward, the Fe<sub>2</sub>O<sub>3</sub> was deposited onto the TiO<sub>2</sub>/FTO using electrodeposition method for 5 minutes, in which the iron sulfate (FeSO<sub>4</sub>) was used as the starting material. The process was carried out using a potentiostat (VersaSTAT 4, Ametek), connected to a working electrode (TiO<sub>2</sub>/FTO), counter electrode (Pt) and reference electrode (Saturated Calomel Electrode, SCE). The samples were calcined in a furnace at 500 °C for 60 minutes with heating rate of 1 °C s<sup>-1</sup>. Characterization of thin films was done using X-Ray diffraction (Bruker D8 Advance) via Cu Kα radiation. Morphology of the thin film was characterized using scanning electron microscopy (Zeiss AM10).

#### Photoelectrochemical analysis

The PEC analysis was conducted based on previous study [17]. The analyses were carried out using Ametek Versastat 4 on the  $TiO_2$  and  $TiO_2$  deposited by  $Fe_2O_3$  at different times. The 450 W full arc Xenon light source at an intensity of 100 mWcm<sup>-2</sup> was used to irradiate the electrodes. The electrolyte in this experiment was 0.5 M  $Na_2SO_4$ , and it was purged with nitrogen gas for 30 min before the tests. The scan rate was set to 0.01 V s<sup>-1</sup>.

#### Computational method

Density functional theory (DFT) calculations were carried out using the DMol<sup>3</sup> code in Materials Studio 5.5 from Accelrys. Geometry of the bulk molecule was optimized in a double-numeric-plus polarization (DNP) basis, set

using three different functional methods: PWC, PW91 and PBE. Self-consistent field (SCF) method was used for calculating the electronic structure; all core electrons were treated as being polarizable and Hartree-Folk (RHF) spin-restricted mode. TDDFT calculations were conducted on the ground state in spin-restricted mode.

# **Results and Discussion**

X-ray diffraction (XRD) patterns of the  $TiO_2$  and  $TiO_2/Fe_2O_3$  on the FTO films are shown in Figure 2. The  $TiO_2$  anatase (101) phase was observed at 25.35°, while rutile (110) phase appeared at 27.40° (Figure 2b). The peaks for  $\alpha$ -Fe<sub>2</sub>O<sub>3</sub> (104) appeared at 33.50°, while  $\alpha$ -Fe<sub>2</sub>O<sub>3</sub> (110) at 35.50° (Figure 2c) (JCPDS file no. 01-077-9926). All  $TiO_2$  and  $Fe_2O_3$  peaks were observed at  $TiO_2/Fe_2O_3$  composite pattern (Figure 2d). Diffractogram pattern of the  $TiO_2$  produced is similar with  $TiO_2$  pattern that was reported by Vlasa et al. [18].

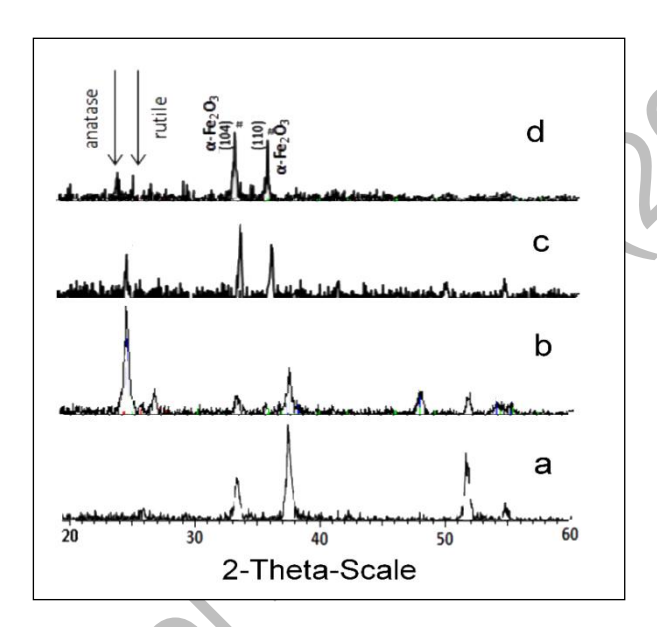


Figure 2. X-ray diffraction for (a) FTO (b) TiO<sub>2</sub> and (c) Fe<sub>2</sub>O<sub>3</sub> and (d) TiO<sub>2</sub>/Fe<sub>2</sub>O<sub>3</sub>

The surface morphology by scanning electron microscopic (SEM) image of  $TiO_2/Fe_2O_3$  on an FTO glass substrate is shown in Figure 3. The image clearly shows flower-like shape on the surface of  $TiO_2$  substrate (B), which is similar to a previous study [19]. The duration of deposition time changed the shape of  $Fe_2O_3$ ; at 3 minutes, the flower-like shape changed to a spiny and globular structure (C) and then turned to fine particles that scattered randomly onto  $TiO_2$  surface at 5 minutes (D). The presence of Fe was confirmed by EDX analysis (Table 2). The number of Fe did not automatically increased with time of deposition; however, the shape of Fe was: at 5 minutes of deposition time, the Fe shape became clotted and the  $TiO_2$  surface became exposed. The thickness of  $TiO_2/Fe_2O_3$  layer on the FTO substrate based on SEM images was obtained around 10-15  $\mu$ m.

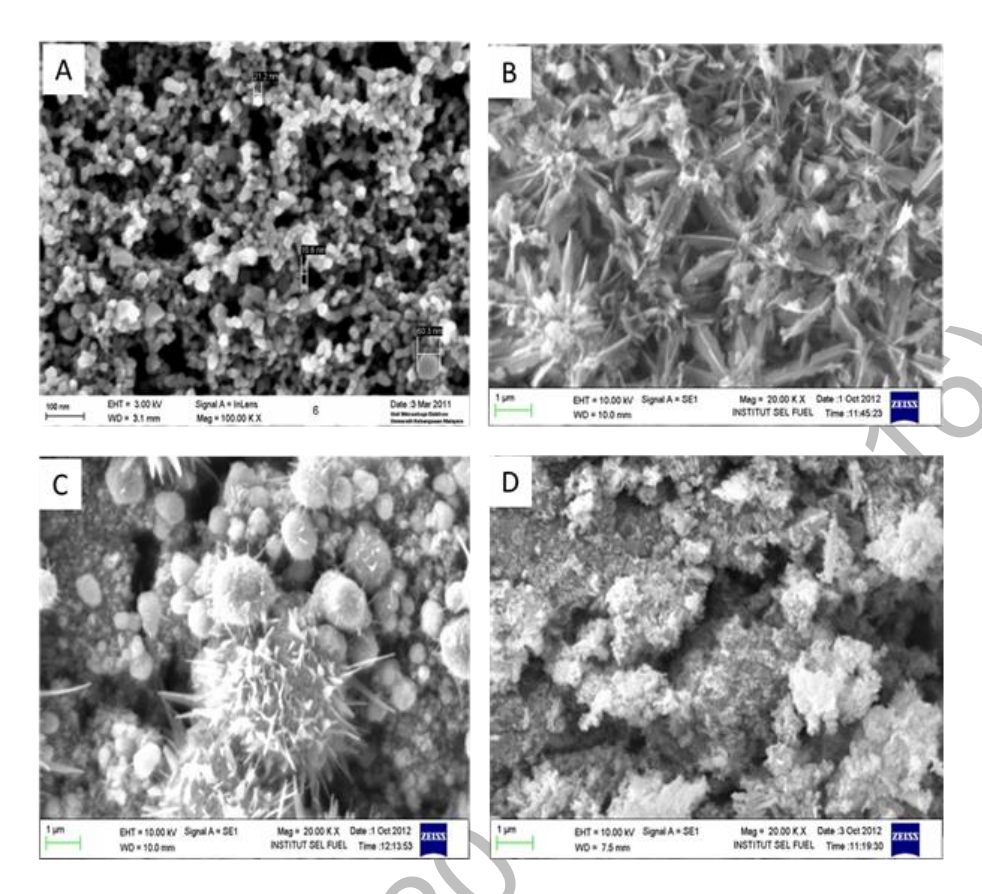


Figure 3. Surface morphology of (a) TiO<sub>2</sub> and (b) TiO<sub>2</sub>/Fe<sub>2</sub>O<sub>3</sub> on FTO films

Table 2. Element percentage of Fe, Ti and O based on EDX analysis

	Percentage (%) of element			
Element	TiO <sub>2</sub> -Fe <sub>2</sub> O <sub>3</sub> (1 min)	TiO <sub>2</sub> -Fe <sub>2</sub> O <sub>3</sub> (3 min)	TiO <sub>2</sub> -Fe <sub>2</sub> O <sub>3</sub> (5 min)	
Ferrum (Fe)	57.0	29.8	16.3	
Titanium (Ti)	55.6	42.8	18.6	
Oxygen (O)	28.2	27.4	24.4	

The optical characterizations of TiO<sub>2</sub> and TiO<sub>2</sub> doped Fe<sub>2</sub>O<sub>3</sub> are shown in Figure 4. The band gaps were determined from reflectance spectra of the films using the following formula equation 1[5]:

$$E_{g}(eV) = 1240/\lambda_{g}(nm) \tag{1}$$

where,  $E_g$  and  $\lambda_g$  are the band gap energy and the absorption wavelength threshold of the doping material, respectively. In figure 5, the band gap of TiO<sub>2</sub> was found to be 3.44 eV with the threshold wavelength at 360 nm. On the other hand, band gap of the TiO<sub>2</sub> doped with Fe<sub>2</sub>O<sub>3</sub> was 2.39 eV with the threshold wavelength at 518 nm. The TiO<sub>2</sub>/Fe<sub>2</sub>O<sub>3</sub> film absorption was shifted to visible light, caused by excitation of electrons in the 3d shell of Fe to conduction band of TiO<sub>2</sub> [20].

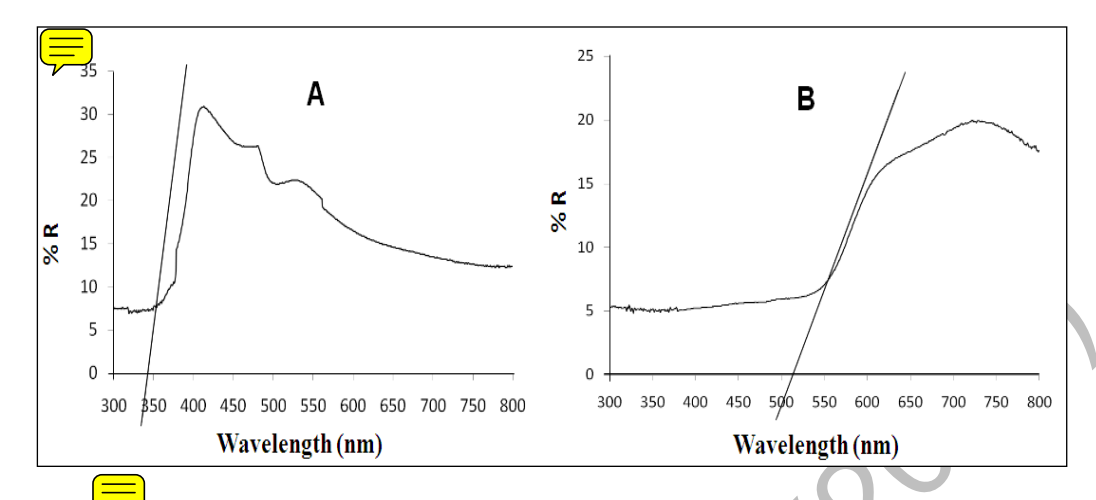


Figure 4. Reflection (R) spectra of TiO<sub>2</sub> and TiO<sub>2</sub> doped Fe<sub>2</sub>O<sub>3</sub> (5 min) electrodes

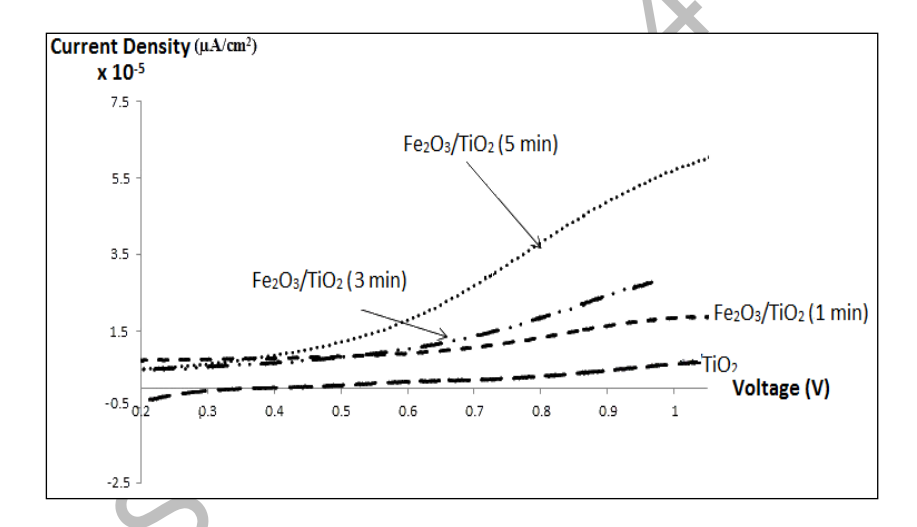


Figure 5. Current density-voltage (V/SCE) characteristics for Fe<sub>2</sub>O<sub>3</sub>/TiO<sub>2</sub> at different duration of electrodeposition proses

Photocurrent density was measured using three electrodes in 0.5 M  $Na_2SO_4$  electrolyte under a Xenon lamp (100 mW cm<sup>2</sup>) irradiation. The applied voltage bias was measured againts SCE as the reference, and the values of photocurrent are shown in Figure 5. The current density of undoped  $TiO_2$  was low compared with  $TiO_2$  doped with  $Fe_2O_3$ . In addition, the deposition time of  $Fe_2O_3$  onto  $TiO_2$  surface contributed to the increase of current density. The highest photocurrent was measured at 5 minutes deposition of  $Fe_2O_3$ , which was about 55  $\mu$ A cm<sup>-2</sup> at 1.0 V bias potential. The current density of  $TiO_2$  without  $Fe_2O_3$  is 7  $\mu$ Acm<sup>-2</sup> and  $TiO_2/Fe_2O_3$  at 1 and 3 minutes are 28  $\mu$ Acm<sup>-2</sup> and 29  $\mu$ Acm<sup>-2</sup>, respectively. This is probably due to the reduction of electron-hole recombination on  $TiO_2$  doped with  $Fe_2O_3$ . Kim et al. found similar result, where the passivation layer of  $TiO_2$  with  $Fe_2O_3$  as photo-absorber on FTO film showed 3.5 times higher photocurrent densities for water splitting under UV-vis light illumination than the  $Fe_2O_3/FTO$  or  $TiO_2/FTO$  films [11].

Theoretical investigation started with the optimization of the bulk structure of  $TiO_2$  and  $Fe_2O_3$  in three kinds of functional methods. The average length of Ti-O and Fe-O are shown in Table 3. Calculated bond length of the Ti-O in these three methods gave similar results, which was about 1.92 Å. The calculated bond length of the Fe-O in PWC was about 0.03 Å smaller than the calculated PW91 and PBE, which was about 1.96 Å. All calculated bond lengths of the Ti-O and Fe-O were in normal range [16]. The band gap of  $TiO_2$  and  $Fe_2O_3$  in these three methods were similar at about 0.076 Ha (2.06 eV) and 0.03 Ha (0.81 eV), respectively (Figure 6). Although the calculated band gaps were smaller than the experimental data, it is aceptable since the calculations were in atomic level.

Table 3.	Bond length (Å	(a) of the optimized	structure in three	different functional	method calculation.
	8 8	,			

Bulk	LDA-PWC	GGA-PW91	GGA-PBE
Ti-O	1,923	1,927	1,927
Fe-O	1,939	1,960	1,960

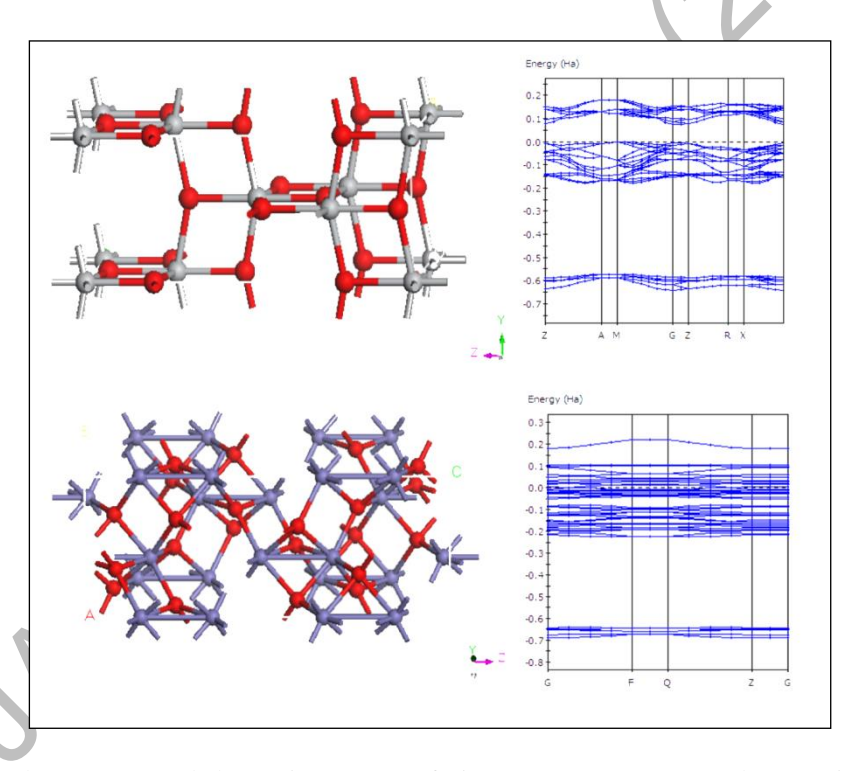


Figure 6. Molecular structure and electronic structure of TiO<sub>2</sub> (101), Fe<sub>2</sub>O<sub>3</sub> (104) and composite TiO<sub>2</sub>/Fe<sub>2</sub>O<sub>3</sub>

The optimized bulk structures of  $TiO_2$  and  $Fe_2O_3$  were used to form  $TiO_2$  (101) and  $Fe_2O_3$  (104) phases, which were then re-optimized further. The molecular structure of  $TiO_2$  (101)/ $Fe_2O_3$  (104) bilayer is shown in Figure 7. The electronic structure of the bilayer can not be determined easily since the increasing atomic number causes overlapping of the electronic orbitals. Nevertheless, band gap of the composite can be determined from the calculation of HOMO-LUMO energy gaps (0.70 eV), which is smaller than the monolayer oxides bad gaps; an indication of the charge transfer improvement in the system. Also shown in Figure 7 the potential electrophilic charge of the composite surface, where the potential of both oxides are similar. The more positive charge was found around Fe atoms, where supposedly the location of oxygen atom oxidation.

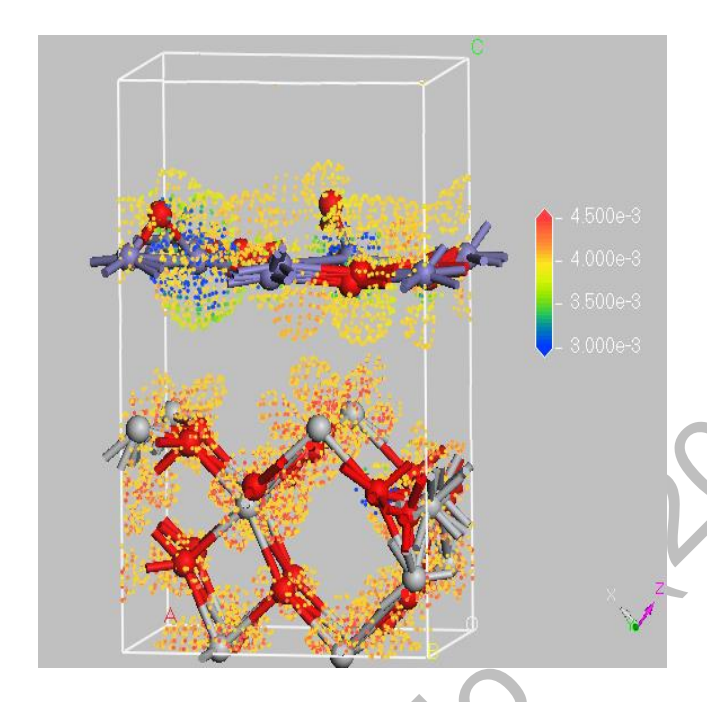


Figure 7. Molecular structure and electrophilic charge of TiO<sub>2</sub> (101)/Fe<sub>2</sub>O<sub>3</sub> (104) composite

#### Conclusion

Surface passivation layer of  $TiO_2/Fe_2O_3$  for use in the PEC water splitting application was successfully fabricated.  $FeSO_4$  was used as the starting material and electrodeposition technique was used to deposit the iron molecule onto  $TiO_2$  thin film. The measurements from photocurrent and reflection spectrum showed that  $Fe_2O_3$  increased the performance of  $TiO_2$  electrode. The maximum photocurrent was obtained from 5 minutes electrodeposition of  $Fe_2O_3$  on  $TiO_2/FTO$  film. The  $TiO_2/Fe_2O_3$  composite structure was built based on DFT calculations. The potential charges of the composite surface were successfully determined.

#### Acknowledgement

The authors would like to acknowledge Universiti Kebangsaan Malaysia for sponsoring this project under UKM-GUP-2011-369 and UKM-AP-TK-05-2009 research grants.

# References

- 1. Arifin, K., Majlan, E.H., Daud, W. R.W. and Kassim, M.B. (2012). Bimetallic complexes in artificial photosynthesis for hydrogen production: A review. *International Journal of Hydrogen Energy*, 37: 3066 3087.
- 2. Currao, A. (2007) Photoelectrochemical water splitting. *Chimia*, 61: 815 819.
- 3. Liu, R., Zheng, Z., Spurgeon, J. and Yang, X. (2014). Enhanced photoelectrochemical water-splitting performance of semiconductors by surface passivation layers. *Energy and Environmental Science*, 7: 2504 2517.
- 4. Minggu, L. J., Daud, W. R.W. and Kassim, M. B. (2010). An overview of photocells and photoreactors for photoelectrochemical water splitting. *International Journal of Hydrogen Energy*, 3(35): 5233 5244.
- 5. Arifin, K., Daud, W. R.W. and Kassim, M.B. (2013). Optical and photoelectrochemical properties of a TiO<sub>2</sub> thin film doped with a ruthenium-tungsten bimetallic complex. *Ceramics International*, 39: 2699 2707.
- 6. Fujishima, A., Zhang, X. and Tryk, D.A. (2008). TiO<sub>2</sub> photocatalysis and related surface phenomena. *Surface Science Reports*, 63: 515 582.
- 7. Arifin, K., Daud, W. R.W. and Kassim, M.B. (2014). A novel ruthenium-tungsten bimetallic complex dyesensitizer for photoelectrochemical cells application. *Sains Malaysiana*, 43(1): 95 101.

- 8. Ni, M., Leung, M. K. H., Leung, D.Y.C. and Sumathy, K. (2007). A review and recent developments in photocatalytic water-splitting using TiO<sub>2</sub> for hydrogen production. *Renewable and Sustainable Energy Review*, 11: 401 425.
- 9. Lin, F. and Boettcher, S.W. (2013). Adaptive semiconductor/electrocatalyst junctions in water-splitting photoanodes. *Nature Materials*, 13: 81 86.
- 10. Cao, C., Hu, C., Shen, W., Wang, S., Tian, Y. and Wang, X. (2012). Synthesis and characterization of TiO<sub>2</sub>/CdS core–shell nanorod arrays and their photoelectrochemical property. *Journal of Alloys and Compounds* 523: 139 145.
- 11. Kim, B-R., Oh, H-J., Yun, K-S., Jung, S-C., Kang, W. and Kim, S-J. (2013). Effect of TiO<sub>2</sub> supporting layer on Fe<sub>2</sub>O<sub>3</sub> photoanode for efficientwater splitting. *Progress in Organic Coatings*, 76:1869 1873
- 12. Fitzmorris, R. C. and Zhang, J. Z. (2015). Recent advances in metal oxide-based photoelectrochemical hydrogen production. In: Andrews D.L., editors. Photonics, Volume 2: Nanophotonic Structures and Materials, Canada, John Willey & Son. pp 346 358.
- 13. Smith, W., Wolcott, A., Fitzmorris, R. C., Zhang, J. Z. and Zhao, Y. (2011). Quasi-core-shell TiO<sub>2</sub>/WO<sub>3</sub> and WO<sub>3</sub>/TiO<sub>2</sub> nanorod arrays fabricated by glancing angle deposition for solar water splitting. *Journal of Material Chemistry*, 21: 10792 10800.
- 14. Minggu, L. J., Ng, K. H., Kadir, H. A. and Kassim, M. B. (2014). Bilayer n-WO<sub>3</sub>/p-Cu<sub>2</sub>O hotoelectrode with photocurrent enhancement in aqueous electrolyte photoelectrochemical reaction. *Ceramics International*, 40: 16015 16021.
- 15. Wang, Q., Yang, X., Chi, L. and Cui, M. (2013). Photoelectrochemical performance of CdTe sensitized TiO<sub>2</sub> nanotube array photoelectrodes. *Electrochimica Acta*, 91: 330 336.
- 16. Zhong, M., Shi, J., Xiong, F., Zhang, W. and Li, C. (2012). Enhancement of photoelectrochemical activity of nanocrystalline CdS photoanode by surface modification with TiO<sub>2</sub> for hydrogen production and electricity generation. *Solar Energy*, 86: 756 763.
- 17. Hang, N. K., Minggu, L.J. and Kassim, M.B. (2013). Gallium-doped tungsten trioxide thin film photoelectrodes for photoelectrochemical water splitting. *International Journal of Hydrogen Energy*, 38: 9585 9591.
- 18. Vlasa, A., Varvara, S., Pop, A., Bulea, C. and Muresan, L.M. (2010). Electrodeposited Zn–TiO<sub>2</sub> nanocomposite coatings and their corrosion behavior. *Journal of Applied Electrochemistry*, 40: 1519 –1527.
- 19. Zanganeh, S., Torabi, M., Kajbafvala, A., Zanganeh, N., Bayati, M.R., Molaei, R., Zangar, H.R. and Sadrnezhaad, S. K. (2010). CVD fabrication of carbon nanotubes on electrodeposited flower-like Fe nanostructures. *Journal of Alloys & Compounds*, 507: 494 497.
- 20. Khan, M. A., Woo, S. I. and Yang, O-B. (2008). Hydrothermally stabilized Fe(III) doped titania active under visible light for water splitting reaction. *International Journal of Hydrogen Energy*, 33: 5345 –5351.

